**MINISTRY OF EDUCATION AND TRAINING**

**VIET NAM ACADEMY OF SCIENCE AND TECHNOLOGY**

**GRADUATE UNIVERSITY OF SCIENCE AND TECHNOLOGY**


**Do Truc Vy**

# INVESTIGATION INTO THE MANUFACTURING PROCESS AND CHARACTERISTICS OF OPTICAL CIRCUIT SUTURE COATINGS UTILIZING ACRYLATE RESINS AND ZnO-Ag NANOPARTICLES

**SUMMARY OF DISSERTATION ON**

**POLYMOLECULAR AND COMPOSITE MATERIALS**

**Code: 9 44 01 25**

***Ha Noi – 2024***

The project was completed at: Academy of Science and Technology, Viet Nam academy of science and technology

Science instructor:

1. Supervisor 1: Dr. Nguyen Thien Vuong, Institute of Tropical Technology
2. Supervisor 2: Dr. Ngo Thanh Dung, Institute of Tropical Technology

Referee 1: Associate Professor. Nguyen The Huu

Referee 2: Associate Professor. Hoang Mai Ha

Referee 3: Associate Professor. Tran Dinh Trinh

The dissertation is examined by Examination Board of Graduate University of Science and Technology, Vietnam Academy of Science and Technology at 9:00 a.m (August 27, 2024).

The dissertation can be found at:

1. Graduate University of Science and Technology Library
2. National Library of Vietnam

# INTRODUCTION

## 1. Reason for choosing the topic

Organic coatings are extensively utilized for enhancing the surface characteristics of various materials, including metals, woods, plastics, and concretes, while also providing protection against environmental factors. The exploration and advancement of intelligent coatings with self-cleaning and antibacterial functionalities are deemed essential.

Tropical regions exhibit thermal climatic conditions, high levels of ultraviolet radiation, intense humidity, heavy rainfall, and elevated levels of moisture, creating favorable environments for mold and bacterial growth on diverse surfaces like furniture items (e.g., flooring, wall cladding, household appliances), glass doors, and house walls. Consequently, researchers are engaged in the development of innovative materials featuring self-cleaning and antibacterial properties. Recent investigations have indicated that hybrid nanoparticles demonstrate enhanced antibacterial and self-cleaning capabilities compared to their non-hybrid counterparts. Nonetheless, there is a dearth of scholarly publications concerning the utilization of these hybrid nanoparticles in optical circuit suture coatings, as well as studies on their self-cleaning, antibacterial, and weather resistance attributes. Furthermore, limited information exists on the principles governing sequential polymerization and the impact of hybrid nanoparticles on the self-cleaning and antibacterial efficacy of such coatings. The successful realization of this subject matter is expected to yield a scientific contribution by elucidating certain principles of photojunction polymerization and photodegradation in the presence of hybrid nanoparticles, shedding light on the influence of hybrid nanoparticles on the self-cleaning and antibacterial properties of these novel coatings. The thesis research, titled "Fabrication and properties study of optical circuit suture coatings based on acrylate resins and ZnO-Ag hybrid nanoparticles," was conducted in this context.

## 2. Thesis objectives

Tổng hợp thành công hạt nano lai ZnO-Ag, có năng lượng vùng cấm thấp có khả ZnO-Ag hybrid nanoparticles were successfully synthesized, characterized by low bandgap energies conducive to photocatalytic activity across a broad spectrum encompassing ultraviolet and visible light wavelengths. Elucidation of optical circuit stitching polymerization and photodegradation in coatings incorporating ZnO-Ag hybrid nanoparticles

was achieved. The impact of hybrid nanoparticles on various coating properties, including mechanical attributes, self-cleaning capabilities, and antibacterial properties, was thoroughly assessed. This endeavor aspires to make a modest contribution to fundamental scientific knowledge and the potential practical applications in the field.

**3. Research content**

- Synthesis of hybrid ZnO-Ag nanoparticles.
- Investigation of optical circuit stitching of coatings based on acrylate resins and ZnO-Ag hybrid nanoparticles.
- Exploration of the antibacterial properties of optical vascular suture coatings.
- Examination of the self-cleaning capabilities of optical vascular suture coatings.
- Analysis of the photocatalytic attenuation of optical vascular suture coating.

**4. Research Methods**

- *Techniques for the synthesis of materials.*
- *Approaches for structural analysis.*
- *Methodology for testing antimicrobial and self-cleaning activities.*

**5. Scientific and practical significance**

Tropical regions experience a thermal climate, characterized by high levels of ultraviolet radiation, heat, humidity, and heavy rainfall, creating optimal conditions for the growth of mold and bacteria on various surfaces like furniture products, glass doors, and house walls. Consequently, researchers are actively engaged in the development of innovative materials that possess self-cleaning properties and environmentally friendly antibacterial characteristics. Particularly, there is a focus on the utilization of nanoparticles such as a-TiO2 and ZnO in the creation of self-cleaning and antibacterial materials and coatings. The incorporation of silver (Ag) into these materials leads to the formation of a Schottky barrier between Ag and semiconductor oxides like ZnO, as a result of the disparity in conduction band energy levels. This phenomenon inhibits recombination between electrons and voids on the ZnO surface by enabling the transfer of free electrons from ZnO to Ag. The presence of electrons on the Ag nanoparticle

is conducive to the generation of ·O2− free radicals, while voids in the valence band can react with H2O2 to produce ·OH radicals. These radicals exhibit potent reactivity, facilitating the breakdown of organic compounds into CO2 and H2O. Experimental findings have demonstrated that ZnO-Ag hybrid nanoparticles exhibit superior photocatalytic activity compared to ZnO particles alone. Thus, the successful synthesis of ZnO-Ag hybrid nanoparticles with enhanced photocatalytic properties, and their subsequent application in the development of optical circuit suture coatings based on self-cleaning and antibacterial acrylate resins, holds significant scientific and practical implications.

**6. New contributions of the thesis**

ZnO-Ag hybrid nanoparticles were effectively produced through the process of thermal decomposition in organic solvents. The synthetic ZnO-Ag hybrid nanoparticles exhibit a band gap energy of 2.6 eV, which is lower compared to pure ZnO (3.2 eV). They demonstrate remarkable photocatalytic performance across a broad spectrum, encompassing both ultraviolet and visible light regions. Moreover, these nanoparticles disperse effectively in nonpolar solvent systems due to the presence of oleyamine surfactant on their surface.

ZnO-Ag hybrid nanoparticles play a crucial role in facilitating optical circuit stitching reactions and promoting the photo-catalytic degradation of coatings.

The incorporation of ZnO-Ag nanoparticles with a content of less than or equal to 2% enhances the mechanical characteristics of coatings. Coatings based on acrylate resin containing 2% ZnO-Ag hybrid nanoparticles exhibit notable antibacterial and self-cleaning properties.

**7. Layout of the thesis**

The thesis structure comprises three chapters and concluding and critical sections:

Chapter 1: Overview of Acrylic Paint and Silver Nanoparticles

Chapter 2: Experiments and Research Methods

Chapter 3: Results and Discussion

Presentation of findings and their implications.

# CHAPTER 1. OVERVIEW

The overview integrates domestic and international research on the subject matter.

***1.1. Lớp phủ khâu mạch quang trên cơ sở nhựa acrylate và hạt nano***

***1.2. Exploration of self-cleaning and antibacterial properties in coatings.***

***1.3. Evaluation of weathering deterioration of the coating in the presence of photocatalytic compounds.***

# CHAPTER 2: EXPERIMENTAL

## 2.1. Materials

## 2.2. The synthesis process involves ZnO-Ag hybrid nanoparticles.

Hybrid ZnO-Ag nanoparticles are synthesized using two distinct methods: thermal decomposition in organic solvents and chemical reduction in an aqueous medium.

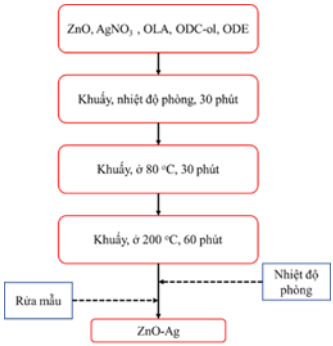


*Figure 2.1: Synthesis of hybrid ZnO-Ag nanoparticles through the thermal decomposition method in organic solvents.*

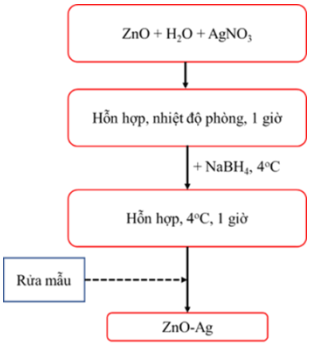


*Figure 2.2: Process for the synthesis of hybrid ZnO-Ag nanoparticles via chemical reduction.*

## 2.3. The concentrate of hybrid ZnO-Ag nanoparticles is essential for the fabrication process.

To prepare synthetic ZnO-Ag nanoparticles and HDDA diluent, the mixture is subjected to ultrasonic vibration for 60 minutes followed by stirring at 1200 rpm for 30 minutes. Subsequently, E284 resin or BGDM

resin is gradually added to the mixture, which is then vibrated for 60 minutes and stirred at the same speed for another 60 minutes. Finally, the photoinitiator I.184 is introduced and the mixture is stirred (in the absence of light) until fully dissolved.

Post-preparation, a film is fabricated on glass and steel plates of the ERICHSEN MODEL 360 equipment with an appropriate thickness for conducting various tests. The membrane samples are then exposed to UV irradiation at specific intervals, up to a maximum of 4.8s, with machine transmission tape speeds set at 40m/s and 5m/s to carry out circuit stitching.

**2.4. Experimental analysis methods**

- Transmission Electron Microscopy (TEM) images are captured using a JEOL TEM transmission electron microscope at the Central Institute of Hygiene and Epidemiology, employing a voltage range of 40 - 100 kV and achieving a pixel resolution of 0.2 nm.

- Scanning Electron Microscope (FESEM) images are obtained utilizing the S-4800 (Hitachi) instrument at the Institute of Materials Science, Vietnam Academy of Science and Technology.

X-ray Diffraction (XRD) analysis is performed on a SIEMENS D5005 - Bruker X-ray diffractometer using Cu-kα radiation ($\lambda$ = 1.5406 Å) at the Department of Physics, University of Natural Sciences, Hanoi National University.

- The utilization of the UV-VIS diffused reflector spectrum is implemented on the UV light meter Vis 2600 by Shimadzu at the Institute of Physics, Vietnam Academy of Science and Technology.

- Energy dispersion spectrum (EDX) examination of the chemical composition of specimens carried out on the SEM-EDX scanning electron microscope (Jeol 6490 — JED 2300, Japan), Institute of Materials Science, Vietnam Academy of Science and Technology.

- Infrared spectroscopic analysis conducted using the FTIR instrument, NEXUS 670, Nicolet (USA) at the Institute of Tropical Engineering, Vietnam Academy of Science and Technology.

- The determination of the gel portion

- Evaluation of the mechanical characteristics of membranes

- The process employed for assessing the antibacterial efficacy of the coating involves the colony counting method, as stipulated in TCVN

9064:2012, which is executed at the Institute of Biotechnology, Vietnam Academy of Science and Technology.

- The technique utilized for evaluating the self-cleaning capability of the coating

## CHAPTER 3: RESULTS AND DISCUSSION

### 3.1. Characteristics of Zno-Ag hybrid nano particles

#### *3.1.1. Characterization of Thermodegradable ZnO-Ag Hybrid Nanoparticles in Organic Solvents (ZA1) is conducted.*

*3.1.1.1. The morphology of ZA1 nanoparticles is carefully examined.*

Figure 3.1 illustrates the initial ZnO particle possessing an elongated cylindrical structure, measuring 50 - 100 nm. Subsequent to silver reduction, diminutive spherical Ag nanoparticles are observed to be deposited on the surface of the ZnO particles. Analysis of TEM images of hybrid nanoparticles reveals that the mean size of the Ag particle affixed to the surface of ZnO particles is approximately 8.1 + 0.2 nm

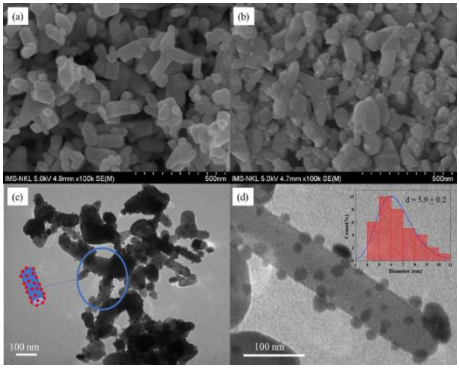


*Figure 3.1: FE-SEM images of ZnO nanoparticles (a) and ZA1 (b); TEM image of ZA1 hybrid nanoparticles (c) and size distribution of Ag nanoparticles (d)*

*3.1.1.2. Analysis of the crystal phase structure and forbidden zone energy of ZA1 nanoparticles is performed.*

XRD patterns of both particle specimens (ZA1 nano and ZnO nano) manifest diffraction peaks at angular positions 2q = 31.77 °, 34.41 °, 36.27 °, 47.57°, 56.63°, 62.92°, 66.39 °, 67.97 °, 69.11 °, 72.60 °, 77.03 ° corresponding

to crystal lattices (100), (002), (101), (102), (110), (103), (200) (112), (201) of ZnO particles (JCPDS No. 36-1451). In the XRD pattern of the Zno-Ag hybrid nanoparticle sample, supplementary diffraction peaks emerge at angular positions 2q = 27.36º, 38.12º, 44.3º, 64.53º, 77.25º corresponding to the lattice planes (210), (111), (200), (220), and (311) in the face-centered cubic structure of Ag (JCPDS No. 04-0783). The average crystal size of Ag nanoparticles computed based on the Scherrer equation is 8.3 nm.

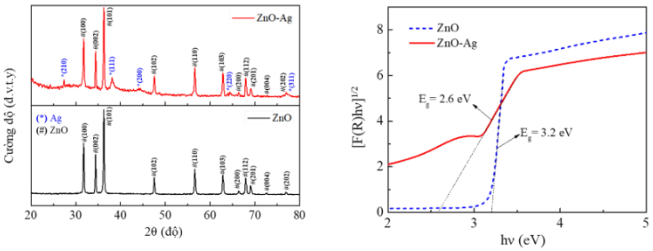


Hình a Hình b

*Figure 3.2: a) X-ray diffraction (XRD) pattern; Figure b) Relationship between function [F(R)hν]$^2$ and band gap energy (hυ) of ZA1 and ZnO particles*

Figure 3.2b indicates that the band gap energy of ZA1 is 2.6 eV, significantly lower than that of the corresponding ZnO nanoparticle's band gap energy of 3.2 eV. Consequently, ZA1 nanoparticles have considerably enhanced their light absorption capacity in the visible spectrum, thereby augmenting the photocatalytic performance of the material in the visible light range.

*3.1.1.4. The Ag content in ZA1 Nanoparticles is analyzed thoroughly.*

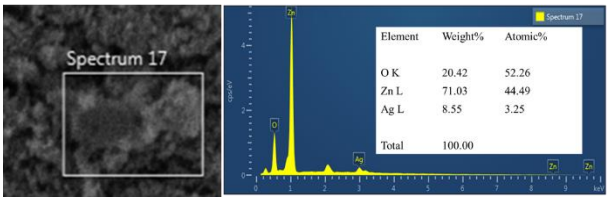


*Figure 3.3: EDX spectrum of ZA1 particles*

The analysis results depicted in figure 3.5 reveal that the thermally degraded ZnO-Ag hybrid nanoparticles primarily consist of Zn, O, and Ag elements, with the element Ag constituting 8.5% of the hybrid system.

### *3.1.2. Đặc trưng của hạt nano lai ZnO-Ag tổng hợp bằng phương pháp khử hóa học trong môi trường nước (ZA2)*

*3.1.2.1. The morphology of ZA2 nanoparticles is carefully examined.*

Figure 3.4 illustrates chemically reduced Ag nanoparticles with a spherical shape, ranging from 10 to 40 nm in size (with an average size of approximately 24 ± 0.6 nm), adhering to the surface of ZnO nanoparticles. The Ag nanoparticles encircling the ZnO nanoparticle surface create core-satellite hybrid structures.

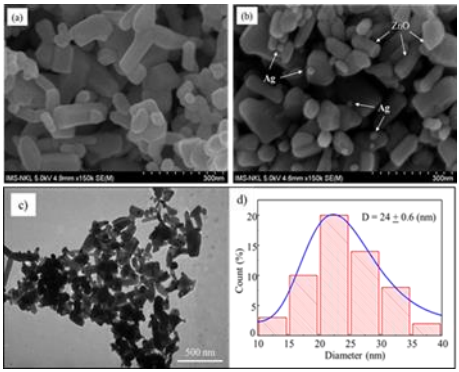


*Figure 3.4: FE-SEM images of ZnO (a) and ZA2 (b) nanoparticles; TEM image of ZA2 nanoparticles (c) and size distribution of Ag nanoparticles (d)*

*3.1.2.2. Analysis of the crystal phase structure and forbidden zone energy of ZA2 nanoparticles is performed.*

The XRD patterns of both samples exhibit diffraction peaks at specific angular positions, including 2θ = 31.77°, 34.41°, 36.27°, 47.57°, 56.63°, 62.92°, 66.39°, 67.97°, 69.11°, 72.60°, 77.03°, corresponding to various crystal lattices of ZnO particles. The XRD analysis of ZnO nanoparticles shows characteristic spectral lines of the hexagonal crystal structure of pure ZnO compounds, without any impurity peaks. Additionally, the XRD pattern of ZA2 displays diffraction peaks at 2θ = 27.36°, 38.12°, 44.3°, 64.53°, 77.25°, corresponding to lattice planes in the face-centered cubic structure of Ag. The average crystal size of Ag nanoparticles is calculated to be 25 nm using the Scherrer formula.

Figure b illustrates that the bandgap energy of ZA2 nanoparticles is measured at 2.75 eV, which is lower than that of ZnO nanoparticles (3.2 eV) but higher than ZA1 hybrid nanoparticles (2.6 eV) as shown in figure 3.5.

This difference may be attributed to the enhanced hybridization of Ag with ZnO in thermal decomposition processes using organic solvents.

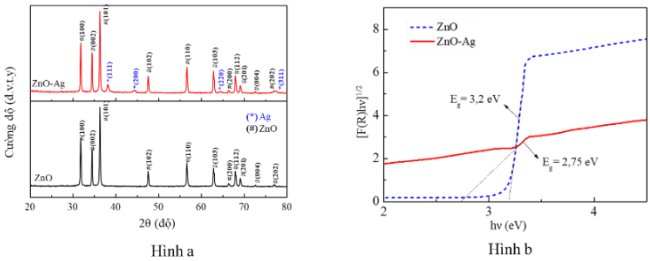


*Figure 3.5: a) X-ray diffraction (XRD) pattern; Figure b) Relationship between function $[F(R)hv]^2$ and band gap energy (hυ) of ZA2 and ZnO particles*

*3.1.2.3. The Ag content in ZA2 Nanoparticles is analyzed thoroughly.*

The analysis results from Figure 3.6 indicate that ZA2 nanoparticles primarily consist of Zn, O, and Ag elements, with the Ag content in the chemically reduced ZnO-Ag hybrid nanoparticles amounting to 5.24%. This percentage is notably lower than the Ag content in ZA1 hybrid nanoparticles (8.5%), suggesting a more effective attachment of Ag to ZnO nanoparticles in thermal decomposition methods using organic solvents.

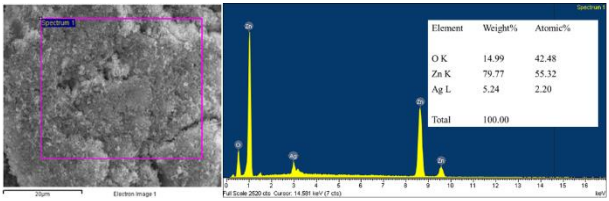


*Figure 3.6: EDX spectrum of ZA2 particles*

** Characterization of synthetic Zno-Ag hybrid nanoparticles is presented via two methodologies: thermal decomposition in an organic solvent and chemical reduction in an aqueous medium, as delineated in Table 3.1.*

*Table 3.1 Some characteristics of thermally decomposed and chemically reduced ZnO-Ag hybrid nanoparticles*

| TT | Đặc tính | ZA1 | ZA2 |
|---|---|---|---|
| 1 | Ag nanoparticle shape | Spherical | Spherical |

| | | | |
|---|---|---|---|
| 2 | Ag nanoparticle size | 8,1 ± 0,2 nm | 24 ± 0,6 nm |
| 3 | Hybrid structural shape | Core-satellistes | Core-satellistes |
| 4 | Bandgap | 2,6 eV | 2,75 eV |
| 5 | Ag content | 8,5% | 5,24% |
| 6 | Dispersion ability | Does not disperse in water, disperses well in organic solvents | Dispersible in water, poorly dispersible in organic solvents |

**3.2. The characteristics of optical circuit suture coatings are determined based on acrylate resins and ZnO-Ag hybrid nanoparticles.**

**3.2.1. Optical circuit stitching of coatings is achieved using acrylate resins and ZnO-Ag hybrid nanoparticles.**

***3.2.1.1. Optical circuit stitching of coatings is achieved using acrylate resins and ZnO-Ag hybrid nanoparticles.***

The kinetics of acrylate groups' metabolism exhibit a rapid initial phase lasting 0.15 s, followed by deceleration, as illustrated in Figures 3.7 and 3.8. Incorporation of 2% ZnO-Ag hybrid nanoparticles (UVAE/ZnO-Ag, UVAU/ZnO-Ag) in coatings amplifies acrylate double bond metabolism compared to formulations lacking ZnO-Ag nanoparticles (UVAE, UVAU). Subsequent to 4.8 s of UV exposure, a significant portion of acrylate double bonds undergo metabolism: 87.24% and 90.39% for epoxy acrylate coatings devoid of ZnO-Ag nanoparticles (UVAE) and those containing 2% ZnO-Ag nanoparticles (UVAE/ZnO-Ag), and 93.53% and 95.82% for urethane acrylate coatings lacking ZnO-hybrid nanoparticles (UVAU) and incorporating 2% ZnO-Ag hybrid nanoparticles (UVAU/ZnO-Ag). Consequently, the presence of ZnO-Ag nanoparticles heightens the metabolism of acrylate double bonds.

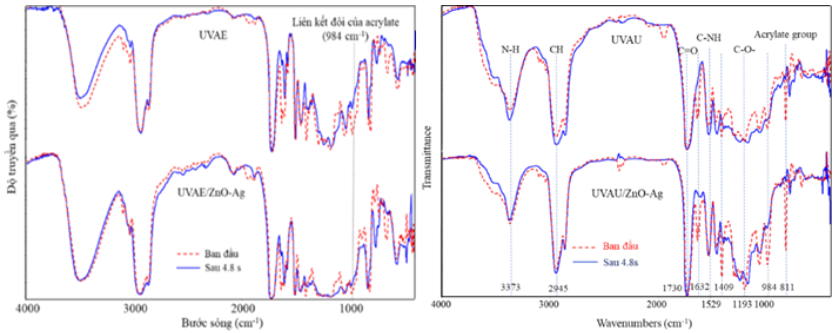


*Figure 3.7: Infrared spectra of (UVAE and UVAE/ZnO-Ag) and (UVAU and UVAU/ZnO-Ag) coatings before and after 4.8 s of ultraviolet radiation*

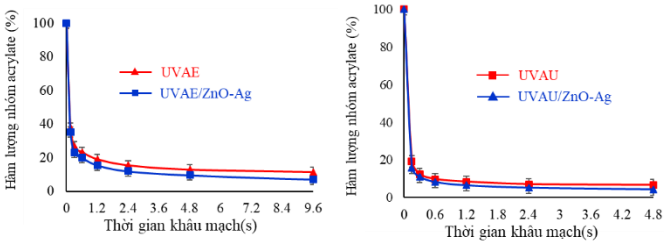


*Figure 3.8: Residual acrylate group content of (UVAE and UVAE/ZnO-Ag) and (UVAU and UVAU/ZnO-Ag) coatings during curing*

### *3.2.1.2. Gel fraction variation and relative hardness of optical circuit suture coatings are measured based on ZnO-Ag hybrid acrylate resins and nanoparticles.*

Examination of Figure 3.9 reveals the emergence of the gel component in the coating at 0.3s under UV radiation. The gel fraction experiences rapid augmentation within the initial 2.4s of UV irradiation, followed by a deceleration in growth rate. By the end of 4.8s of UV exposure, the gel fraction nearly attains peak levels of approximately 95.45% and 96.53% for coatings (UVAE) and UVAE/ZnO-Ag, correspondingly. The outcomes of gel fraction analysis in urethane acrylate (UVAU) and UVAU/ZnO-Ag resin systems are delineated. This data demonstrates that following 0.3s of ultraviolet irradiation, the gel component in both the non-ZnO-Ag-containing and hybrid nanoparticle-containing coatings start to manifest. The gel fraction in both types of coatings undergoes swift escalation within the initial 1.2s, followed by deceleration, with the gel fraction in the

UVAU/ZnO-Ag coating exhibiting a faster increase than that in the UVAU coating. After 4.8s of UV exposure, the gel component in the coating achieves peak values of around 95.3% for UVAU coatings and 96.7% for UVAU/Zno-Ag coatings. Noticeably, the incorporation of ZnO-Ag hybrid nanoparticles results in an elevation of the gel fraction value in the coating, which can be attributed to the contribution of Zno-Ag hybrid nanoparticles' photocatalytic activity.

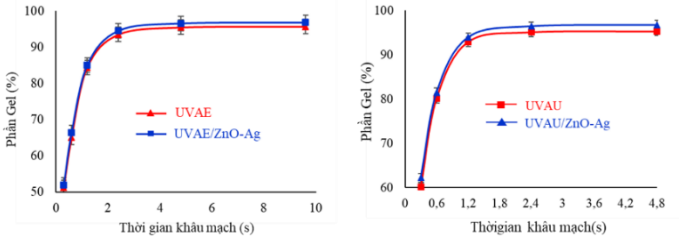


*Figure 3.9: Variations of the gel portion of the coating (UVAE and UVAE/ZnO-Ag) and coating (UVAU and UVAU/ZnO-Ag) during the photocuring process*

Figure 3.10 illustrates the rapid increase in relative hardness of the coating within the initial 1.2 seconds of ultraviolet irradiation, followed by a slower rate of increase in the subsequent 3.6 seconds. Upon reaching 4.8 seconds of UV irradiation, the relative hardness peaks at approximately 0.9 and 0.94 for UVAE coating and UVAE/ZnO-Ag coating, respectively. Conversely, the UVAU/ZnO-Ag coating exhibits a higher hardness value, with peaks of about 0.72 and 0.76 compared to UVAU coating and UVAU/ZnO-Ag coating, respectively. Beyond 4.8 seconds, there is minimal further increase in coating hardness. Hence, the incorporation of an additional 2% ZnO-Ag hybrid nanoparticles into the membrane serves to enhance the relative hardness of the coating.

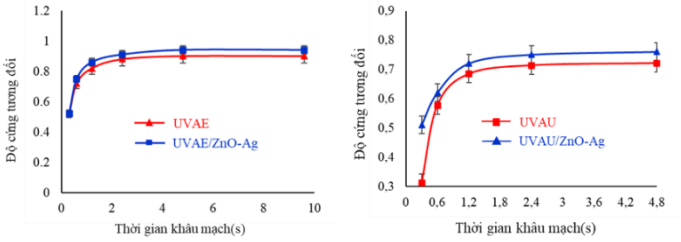

*Figure 3.10: Change in relative hardness of the coating (UVAE and UVAE/ZnO-Ag) and coating (UVAU and UVAU/ZnO-Ag) during the photocuring process*

### 3.2.2. The morphology of ZnO-Ag hybrid nanoparticle optical circuit suture coatings is observed.

Figure 3.11 depicts the compact structure of the coating, devoid of cracks and defects, upon introduction of hybrid nanoparticles into the membrane. These nanoparticles exhibit good dispersion in polymer substrates, ranging in size from 50-200 nm, without forming large clumps. The effective dispersion of hybrid nanoparticles can be attributed to the surrounding oleylamine surfactants on their surfaces, facilitating dispersion within the initial liquid resin mixture.

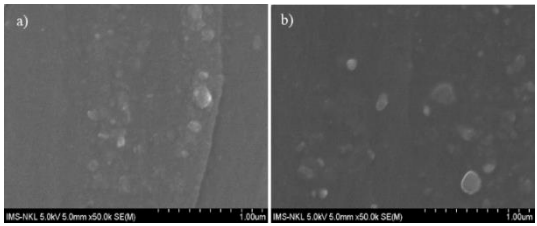


*Figure 3.11: Cross-sectional FE-SEM images of optical cross-linking coatings containing 2% ZnO-Ag nanoparticles: UVAE/ZnO-Ag (a) and UVAU/ZnO-Ag (b)*

### 3.2.3. The mechanical properties of optical circuit suture coatings are influenced by hybrid nanoparticles.

*Table 3.2 Influence of ZnO-Ag hybrid nanoparticle content on the mechanical properties of coatings based on epoxy acrylate resins*

| No | Physical properties | ZnO-Ag hybrid nanoparticle content in the coating, % | | | | |
|---|---|---|---|---|---|---|
| | | 0 | 0,5 | 1 | 2 | 4 |
| 1 | Impact resistance, Kg.cm | 40 | 45 | 50 | 60 | 45 |
| 2 | Abrasion resistance, L/mil | 98,7 | 110,5 | 121,3 | 131,6 | 105,2 |
| 3 | Relative hardness | 0,90 | 0,91 | 0,92 | 0,94 | 0,91 |

*Table 3.3 Influence of ZnO-Ag hybrid nanoparticle content on the mechanical properties of coatings based on urethane acrylate resins*

| No | Physical properties | ZnO-Ag hybrid nanoparticle content in the coating, % | | | | |
|---|---|---|---|---|---|---|
| | | 0 | 0,5 | 1 | 2 | 4 |
| 1 | Impact resistance, Kg.cm | 30 | 40 | 45 | 50 | 40 |
| 2 | Abrasion resistance, L/mil | 95,3 | 99,8 | 112,7 | 121,5 | 96,7 |
| 3 | Relative hardness | 0,72 | 0,74 | 0,75 | 0,76 | 0,73 |

The enhancement of mechanical properties in the coating upon addition of ZnO-Ag hybrid nanoparticles to the polymer substrate can be attributed to two primary factors: firstly, the solid nature of the hybrid nanoparticles, possessing elevated mechanical strength, potentially reinforces the coating. Secondly, these nanoparticles may fill defects within the coating matrix, contributing to the observed improvement in mechanical properties as nanoparticle content increases from zero to 2% by mass. However, at higher concentrations, hybrid nanoparticles tend to agglomerate, diminishing the interaction force between nanoparticles and the polymer substrate, thus leading to a decline in mechanical properties of the coating. Moreover, a hybrid nanoparticle content exceeding 2% results in excessive surface roughness of the coating, elevating frictional forces on the pendulum spheres of the relative hardness measuring instrument, consequently causing a reduction in the relative hardness of the coating.

### 3.2.4. The antibacterial activity of UVAE/ZnO-Ag optical circuit suture coating is evaluated.

After 7 hours of exposure to UVAE coating and UVAE/ZnO coating in the culture solution, there was only a slight reduction in the number of bacteria present on the plate. In contrast, the UVAE/ZnO-Ag coating sample did not show the presence of E. coli bacteria. Upon resuming the test after 24 hours, the number of bacteria in the UVAE coating samples almost plateaued, whereas the UVAE/ZnO coating (with 2% ZnO nanoparticles) continued to decrease to 72 CFU/ml. The specific antibacterial activity values can be found in table 3.4.

*Bảng 3.2 Number of E. coli bacteria at baseline, after 7 and 24 hours of testing.*

| No | Sample | % nano particles | Number of E. coli bacteria (CFU/ml) | | |
|---|---|---|---|---|---|
| | | | Before | After 7h | After 24h |
| 1 | Control sample | 0 | $3,4 \times 10^4$ | $3.8 \times 10^4$ | $2,5 \times 10^3$ |
| 2 | UVAE | 0 | $3,4 \times 10^4$ | $2,6 \times 10^4$ | $2,5 \times 10^3$ |
| 2 | UVAE/ZnO | 2 | $3,4 \times 10^4$ | $1,2 \times 10^3$ | 72 |
| 3 | UVAE/ZnO-Ag | 2 | $3,4 \times 10^4$ | 0 | 0 |

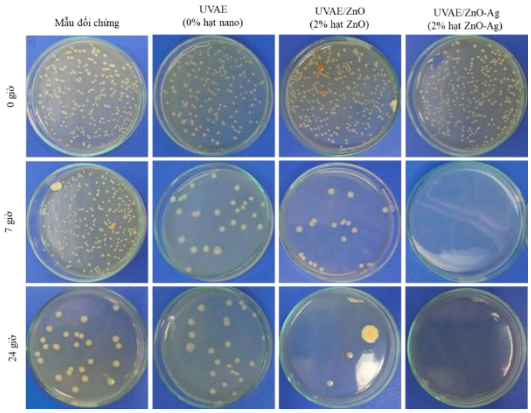


*Figure 3.12: Photos of antibacterial test samples at 0 hour, 7 hour and 24 hour time of experiment*

### *3.2.5. Self-cleaning ability of UVAU/ZnO-Ag optical circuit suture coating is investigated.*

A Methylene Blue (MB) self-cleaning dirt test was carried out on UVAU coatings simultaneously for comparison purposes. The results indicated that MB dirt on the surface of the UVAU/ZnO-Ag coating was almost completely eradicated after 12 hours of ultraviolet irradiation, while the stain remained noticeable on the UVAU coating surface.

The UV-Vis spectrum of the UVAU/ZnO-Ag coating with an MB layer was examined before and after 12 hours of ultraviolet irradiation, as depicted in Figure 3.13. Similarly, the UV-Vis spectrum of the UVAU coating with an MB layer was analyzed before and after 12 hours of ultraviolet irradiation,

shown in Figure 3.14. Analysis of the figures reveals that the characteristic MB absorption in the 500-700 nm range significantly diminishes after 12 hours of ultraviolet irradiation for the UVAU/ZnO-Ag coating (Figure 3.14), while only slightly decreasing for the UVAU-coated sample (Figure 3.23), reaffirming the self-cleaning efficacy of the coating containing 2% ZnO-Ag hybrid nanoparticles.

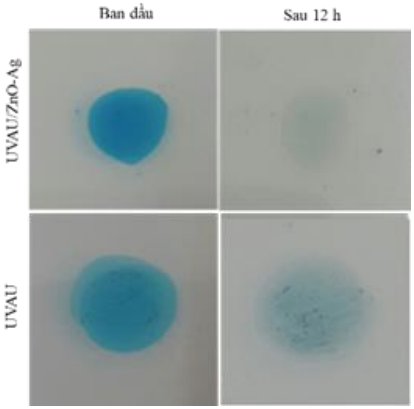


*Figure 3.13: UVAU/ZnO-Ag and UVAU coatings covered with initial MB dirt and after 12 hours of UV irradiation*

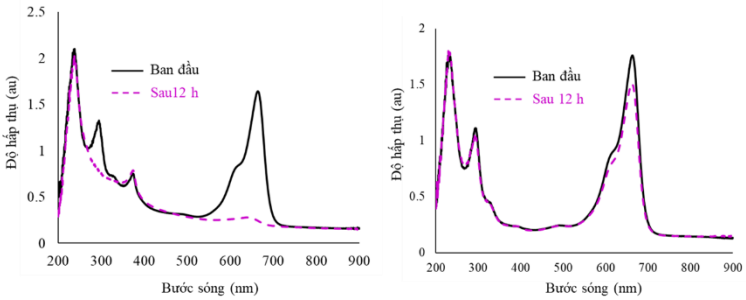


*Figure 3.14: UV-vis spectra of UVAU/ZnO-Ag (a) and UVAU (b) coatings coated with MB dirt initially and after 12 hours of exposure to ultraviolet radiation.*

Photographs illustrating UVAU/ZnO-Ag coating samples coated with artificial dirt mixture before and after 32, 64, and 112 hours of ultraviolet exposure can be seen in Figure 3.15. The artificial dirt mixture was also applied to the UVAU coating surface for comparative testing. Concurrently, the mass loss of the artificial dirt mixture during ultraviolet exposure was monitored, and the results are presented in Figure 3.16.

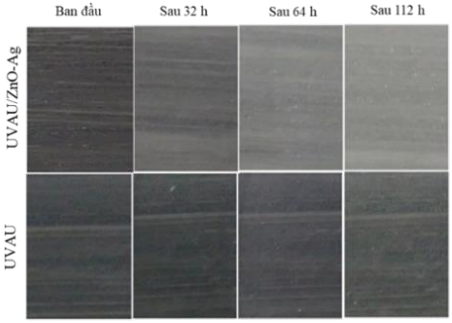


*Figure 3.15: The surfaces of the coating samples were initially covered with artificial dirt and after 32, 64 and 112 h of UV exposure.*

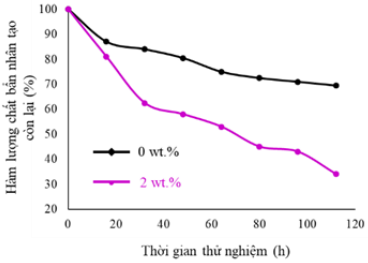


*Figure 3.16: Attenuation of artificial contaminants during ultraviolet radiation testing*

Observing Figure 3.15, it is evident that the dark color of the artificial dirt mixture on the UVAU/ZnO-Ag coating surface diminishes significantly with prolonged exposure to ultraviolet rays, while the color change on the UVAU coating surface is minimal.

In Figure 3.16, it is evident that following 112 hours of ultraviolet exposure, in the presence of ZnO-Ag hybrid nanoparticles, approximately 35% of the artificial dirt mixture remains on the UVAU/ZnO-Ag coating surface while almost 70% persists on the UVAU coating. Consequently, the inclusion of ZnO-Ag hybrid nanoparticles has significantly enhanced the self-cleaning attributes of urethane acrylate coatings. During UV/CON acceleration testing, the self-cleaning mechanism of the coating may entail the photocatalytic disintegration of the substrate polymer by the photocatalytic hybrid nanoparticles, causing a detachment between the dirt and the coating surface, leading to the self-peeling off of dirt from the coating surface.

### 3.2.6. Photocatalytic Weathering Attenuation of UVAU/ZnO-Ag Optical Circuit Suture Coating is studied.

As illustrated in Figure 3.17, a visual examination before the surface evaluation demonstrates relatively uniform coatings. However, subsequent to 48 aging cycles, the coatings exhibit a rougher surface texture. The UVAU coating surface displays a powdery phenomenon, while the UVAU/ZnO-Ag coating surface exhibits abrasion, revealing the presence of hybrid nanoparticles.

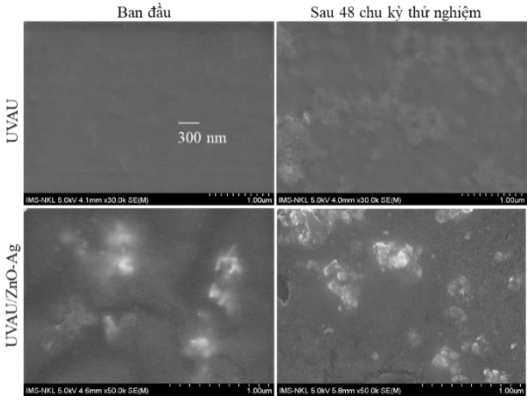


*Figure 3.17: FE-SEM images of initial UVAU and UVAU/ZnO-Ag coatings and after 48h accelerated weathering test*

Figure 3.18 showcases a slight reduction in the intensity of certain absorption bands for UVAU coatings. Conversely, an enhancement in the intensity of the absorption band at 1620 cm-1 is noticeable in the UVAU/ZnO-Ag coating post the aging examination.

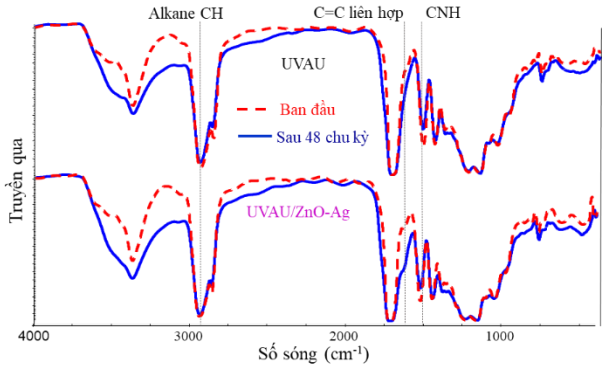


*Hình 3.18: Infrared spectra of UVAU and UVAU/ZnO-Ag coatings initially and after 48 cycles of accelerated weathering testing*

Observations from Figures 3.18 and 3.19 depict a decline in the intensity of the C-H characteristic absorption band (in the alkane group) following the aging test for both coating specimens, with a more pronounced decrease observed in the UVAU/ZnO-Ag coating. This phenomenon could be attributed to a potential reduction in alkane group content during the acceleration test, accompanied by the generation of new carboxyl groups.

Moreover, as indicated in Figure 3.19, an increase in the content of conjugated C=C groups is noted with prolonged weather-attenuation test time for both coatings, with a more significant rise observed in the case of UVAU/ZnO-Ag coatings.

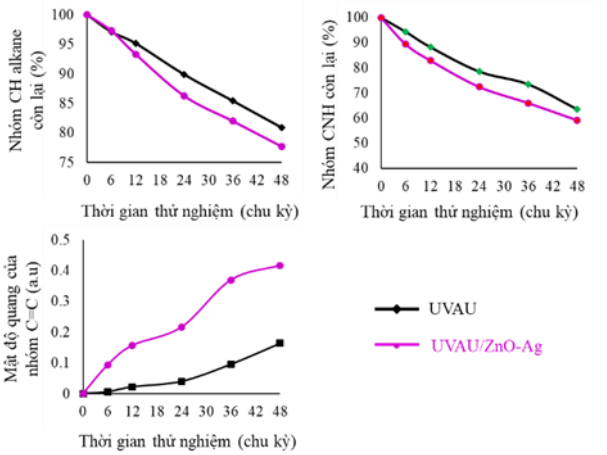


*Hình 3.19: Changes in functional groups in UVAU and UVAU/ZnO-Ag coatings during accelerated weathering testing*

The inclusion of 2% Zno-Ag hybrid nanoparticles in the coating matrix resulted in a notable increase in the weight reduction percentage, reaching approximately 8.3% after 48 test cycles. Conversely, the hybrid non-nanoparticle UVAU coating experienced a weight gain in the initial 12 cycles, followed by a decrease leading to a 6% loss after 48 cycles. During accelerated testing, photo-oxidation and hydrolysis processes can lead to the deterioration of functional groups within the coating, yielding low molecular weight compounds and new functional groups. This research highlights how the incorporation of ZnO-Ag nano-hybrid material in the coating substrate can impact the modification of functional groups and subsequent weight reduction. The findings regarding mass loss align with the results of infrared spectral analyses on the chemical transformations occurring in coatings.

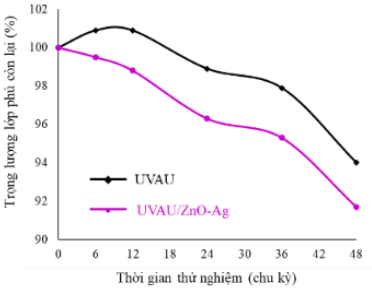


*Hình 3.20: Weight loss of coatings during accelerated weathering testing*

Upon exposure to ultraviolet radiation, ZnO-Ag nanoparticles can be stimulated and subsequently interact with oxygen and H2O, culminating in the formation of the •OH free radical. This hydroxyl radical can engage with the polymer chain through three distinct pathways for photocatalytic disintegration at weak bonds.

In scenario A, the hydroxyl radical has the capability to interact with the polymer chain through two distinct pathways:

(i) Upon interaction, the hydroxyl radical •OH can react with a hydrogen atom in Ca to generate HOH and the carbon radical C•a. Subsequently, another •OH radical may bond with the hydrogen atom in the adjacent carbon atom, resulting in the formation of HOH and a carbon-carbon conjugate double bond compound.

(ii) Following the reaction between the hydroxyl radical •OH and Ca's hydrogen atom, oxygen has the potential to attack the resulting carbon radical C•A, leading to a subsequent increase in the coating's weight.

The prevalence of polymer circuit fragmentation can often obscure clear observations in mass loss analyses (Figure 3.20). Consequently, these processes tend to yield products with lower molecular weights continuously. While both reaction pathways can occur concurrently, their occurrence is dictated by the abundance of •OH radicals. Should the coating follow pathway (i), the reaction rate might be accelerated as aging progresses. Moreover, pathway (ii) could incite a chain reaction. The inclusion of ZnO-Ag is postulated to foster the creation of additional carbon-carbon conjugate double bonds and hydroxyl groups. Consequently, the degradation of the coating is anticipated to proceed via pathway (i) until its completion.

The degradation of the UVAU/ZnO-Ag coating is attributed to the generation of •OH free radicals (induced by ZnO-Ag), potentially leading to an alternative degradation pathway for the pristine coating. This alternative

mechanism may encompass two distinct processes, namely photoxidation (involving O atoms bonding with a polymer substrate) causing an increase in coating weight (as evidenced within the initial 12 cycles of the accelerated test - Figure 3.20); as well as the fragmentation of the polymer chain through photovoltaic/hydrochloric reaction/photocatalysis, resulting in the formation of lower molecular weight byproducts. These byproducts can subsequently be eliminated through evaporation or leaching (via water/moisture), consequently diminishing the mass loss of the coating sample. The weight of the UVAU coating exhibits a gradual decline during the accelerated test, as depicted in Figure 3.20, indicating that the trend (**) will eventually supersede the trend (*).

In scenario B, the •OH free radical can interact with the H atom at C adjacent to the -COO- group, leading to the generation of peroxyl and H2O radicals in the presence of O2. The peroxyl radical promptly engages with the pliable H atom of another polymer chain to facilitate the transfer of the subsequent hydrogen peroxide. This hydrogen peroxide is subsequently disintegrated into lighter compounds, such as aldehydes and CO2, resulting in a reduction of ester and carbonyl bonds, as well as the weight of the polymer coating.

Ultimately, the •OH free radicals may react with the H atom at C neighboring the CNH group, mirroring the polyurethane decomposition mechanism documented elsewhere. This reaction potentially involves the cleavage of hydrogen at the 2nd C atom at the a position of the N atom, resulting in the formation of new substantial molecular free radicals capable of interacting with atmospheric oxygen atoms to generate alkoxy radicals via the establishment/decay of hydroperoxide. The variability in alkoxy radicals may encompass the ability to sever the b circuit and engage in the 'capping' reaction. These two conceivable pathways have the potential to yield a diverse array of photodegradation products, as evidenced by FTIR spectroscopy (Figures 3.18 and 3.19) and mass loss investigations (Figure 3.20).

## CONCLUSIONS

ZnO-Ag hybrid nanoparticles were effectively produced through thermal decomposition in organic solvents. The analytical data pertaining to the characteristics of these hybrid nanoparticles reveal the presence of spherical Ag nanoparticles attached to the ZnO nanoparticles' surface, resulting in Core-Satellistes-type hybrid configurations. The synthesized ZnO-Ag hybrid nanoparticles exhibit a narrower forbidden energy zone of 2.6 eV compared to ZnO's 3.2 eV, enabling robust photocatalytic performance across a broad spectrum encompassing ultraviolet and visible light regions. Due to the encapsulation by the oleyamine surfactant, these nanoparticles disperse efficiently in nonpolar solvents.

The evaluation of the mechanical attributes of optical stitching coatings incorporating 0-4% ZnO-Ag hybrid nanoparticles validated their role as reinforcing fillers enhancing the coating's mechanical properties. The optimal concentration of ZnO-Ag hybrid nanoparticles in the coating was determined to be 2%. For the epoxy acrylate coating, the mechanical properties were found to be at their peak: impact strength of 60 kg.cm, abrasion resistance of 131.6 L/mil, and relative hardness of 0.94. As for the urethane acrylate coating, it exhibited advantages such as impact strength of 95.3 L/mil, abrasion strength of 121.5 L/mil, and double hardness of 0.76.

The optical circuit suture coatings, enriched with 2% ZnO-Ag hybrid nanoparticles, demonstrated notable antibacterial efficacy and efficient self-cleaning properties. Particularly, the epoxy acrylate coating for optical circuit stitching contained 2% ZnO-Ag hybrid nanoparticles that exhibited complete bactericidal activity within a short timeframe (7h). On the other hand, the urethane acrylate coating for optical circuit stitching incorporated 2% ZnO-Ag hybrid nanoparticles capable of nearly complete elimination of methylene blue contaminants after only 12 hours of UV exposure, and cleaning up to 65% of the artificial dirt mixture after 112 hours of UV exposure.

The mechanism underlying optical circuit stitching and the photo-catalytic degradation of the optical circuit suture coating has been elucidated. ZnO-Ag hybrid nanoparticles play a dual role in promoting optical circuit stitching and facilitating the degradation of the coating through weathering simultaneously. The integration of ZnO-Ag hybrid nanoparticles leads to the degradation of the class, favoring the development of p-π conjugated double bond structures.

## LIST OF THE PUBLICATIONS RELATED TO THE DISSERTATION

1. **Do T. V.,** Ha M. N., Nguyen T. A., Ha H. T., Nguyen T. V. - Crosslinking, Mechanical Properties, and Antimicrobial Activity of Photocurable Diacrylate Urethane/ZnO-Ag Nanocomposite Coating. Adsorption Science & Technology, 2021. ($Q_2$/4.4) https://doi.org/10.1155/2021/7387160.
2. Thien Vuong Nguyen, **Truc Vy Do**, Thanh Dung Ngo, Tuan Anh Nguyen, Le Trong Lu, Quoc Trung Vu, Lan Pham Thi and Dai Lam Tran, Photocurable acrylate epoxy/ZnO–Ag nanocomposite coating: fabrication, mechanical and antibacterial properties, RSC Advances 12 (36), 23346-23355, ($Q_2$/4.0) DOI: https://doi.org/10.1039/D2RA03546D
3. **Vy Do Truc**, Thien Vuong Nguyen, Tien Viet Vu, Tuan Anh Nguyen, Thanh Dung Ngo, The Tam Le, Trong Lu Le, Lan Thi Pham, Lam Dai Tran. ZnO− Ag Hybrid Nanoparticles Used in the Antimicrobial Solvent-Based Coatings: Antibacterial Studies in the Darkness and Under Visible-Light Irradiation. ChemistrySelect. 2023 8(6), e202204966. ($Q_2$/2.3) https://doi.org/10.1002/slct.202204966.
4. Nguyen, T.V., **Do Truc, V.,** Nguyen, T.A. et al. A Self-Cleaning UV-Cured Organic Coating with ZnO–Ag Hybrid Nanoparticles. J Clust Sci (2023). ($Q_2$/3.5) https://doi.org/10.1007/s10876-023-02448-1
5. Nguyễn Thiên Vương, **Đỗ Trúc Vy**, "Hạt nano lai ZnO-Ag ưa hữu cơ kháng khuẩn", sở hữu trí tuệ (sáng chế), đã chấp nhận đơn hợp lệ.
6. **Đỗ Trúc Vy**, Nguyễn Thiên Vương, Lê Trọng Lư, Ngô Thanh Dung, Đào Phi Hùng, Trần Đại Lâm, Vũ Quốc Trung, "Quy trình tổng hợp hạt nano lai ZnO-Ag ưa hữu cơ kháng khuẩn", sở hữu trí tuệ (sáng chế), đã chấp nhận đơn hợp lệ.